Chemical Engineering Journal 494 (2024) 153069

Contents lists available at ScienceDirect

Chemical Engineering Journal

journal homepage: www.elsevier.com/locate/cej

# Transforming fabrics into UV-sensing wearables: A photochromic hackmanite coating for repeatable detection

Alicja Lawrynowicz [a,*], Sami Vuori [b], Emilia Palo [a], Mathias Winther [c], Mika Lastusaari [b], Kati Miettunen [a]

[a] Department of Mechanical and Materials Engineering, University of Turku, FI-20014 Turku, Finland
[b] Department of Chemistry, University of Turku, FI-20014 Turku, Finland
[c] Center for Creative Industries & Professions, VIA University College, DK-7400 Herning, Denmark

ARTICLE INFO

*Keywords:*
Hackmanite
Photochromism
Advanced textile
UV-sensing
UV index

ABSTRACT

In this study, we successfully present the first application of a hackmanite coating on a textile substrate to serve as a UV sensor. Photochromic minerals, such as hackmanite, are excellent candidates for designing accurate and long-lasting UV-sensing wearables capable of passively operating without external power sources. By incorporating hackmanites into textiles, UV monitoring can become more accessible and widespread, for example, preventing individuals from sunburn. Here, the resultant photochromic fabric revealed its capacity for swift color changes upon exposure to UV-A and UV-B irradiation, transitioning from white to purple within just 15 s. Subsequent exposure to white light led to a fast, complete reversal of coloration in approximately 50 min. The coloration of the fabric was assessed with reflectance spectroscopy, and the key information (i.e., UV index values) could be read with a proprietary phone app, Sensoglow. This app is designed to provide a convenient analysis of color change with the accuracy of integers values. Additionally, the hackmanite-coated fabric presented exceptional fatigue resistance, retaining consistent coloration across a minimum of 20 photochromic cycles. In contrast, alternative photochromic materials, such as tungstate-or spiropyran-based dyes, showed a gradual decrease in color saturation after just 10 cycles. Moreover, the hackmanite-coated fabric was proficient in monitoring UV index (UVI) values, even at levels below 3, a threshold for taking preventive measures, demonstrating that this fabric serves as a powerful tool for UV-sensing.

## 1. Introduction

Photochromism is the phenomenon in which a material changes color upon absorbing photons of specific wavelengths of light, typically visible light, or ultraviolet (UV) radiation [1,2]. This process is often reversible, allowing the material to return to its original color through, for instance, exposure to white light or heat [1,3,4]. Photochromic materials are employed in a wide range of applications from optical memories and switch to smart textiles due to their properties, such as rapid change of color and remote controllability over long distances using a light source [2–9]. Recent studies have highlighted an increasing interest in utilizing UV-sensitive materials for UV detection [1,2,8,10,11]. Particularly noteworthy is the potential application of photodetectors to textiles, transforming everyday fabrics into practical wearable UV sensors. Such systems hold promise in limiting the risks associated with extended exposure to sunlight or an artificial UV source. By measuring the UV intensity very locally in real time, wearable sensors could play a crucial role in preventing serious conditions, such as skin and eye diseases and cancer [1,8,11–16]. In addition to health benefits, such a UV monitoring feature simply enhances awareness regarding the presence and intensity of harmful UV light, specifically UV-A (315–400 nm) and UV-B (275–315 nm) radiation, since UV-C (200–275 nm) is naturally blocked by the Earth's ozone layer [8,11,17]. Hence, wearable UV sensors offer versatile solutions applicable across all cases that require a UV dosimeter.

Numerous photodetectors, designed for UV monitoring purposes, exhibit good responsiveness and high wavelength discrimination; however, their limitations lie particularly in complex design, which often includes electrical circuits in the system [11,18]. Moreover, the integration of electric circuits into the system presents a significant challenge for washing functional textiles, thereby limiting their potential application in, for example, everyday-use garments. To stabilize

* Corresponding author at: Vesilinnantie 5, 20014 Turku, Finland.
*E-mail address:* alicja.lawrynowicz@utu.fi (A. Lawrynowicz).

https://doi.org/10.1016/j.cej.2024.153069
Received 5 April 2024; Received in revised form 23 May 2024; Accepted 11 June 2024
Available online 12 June 2024

photochromic wearables in the market and facilitate UV-sensing applications, they must be simple and cost-effective [19]. Preferably, photochromic materials should seamlessly blend into existing garments and operate passively, meaning that they require no external energy source while collecting the required dose of the radiation. Thus, one effective method is to directly apply them to textile-based substrates, since this approach simplifies the manufacturing and maintenance processes and eliminates the need to introduce new production techniques [8,20].

The photochromic dyes currently used in the market, including well-researched examples such as spirooxazine, spiropyran, azobenzene, silver nanoparticles, and tungsten and molybdenum oxides, often exhibit toxicity, instability, rare elements, and/or decreased coloration efficiency [1,11,12,20–25]. Their fatigue resistance may also vary depending on usage conditions, such as high temperature or relative humidity [26,27]. Designing durable fabrics from such materials is challenging since textiles need to withstand temperature fluctuations, high humidity, and common fabric treatments like washing and drying, while ensuring chemical safety for both the user and the environment. Moreover, their photochromic life cycle is usually limited, making them incompatible with current market demand and sustainable development expectations, given that long-lasting materials are preferable [8,24,28,29]. For instance, the performance of the reported spiropyran-based photochromic fabric significantly declined after just 10 cycles, and a similar trend was observed with a polyethyleneimine and sodium decadecanate photochromic fabric [30,31]. Photochromic minerals, such as hackmanite ($Na_8Al_6Si_6O_{24}(Cl,S)_2$), can address these problems.

Hackmanites, that is, photochromic sodalites, are well known for

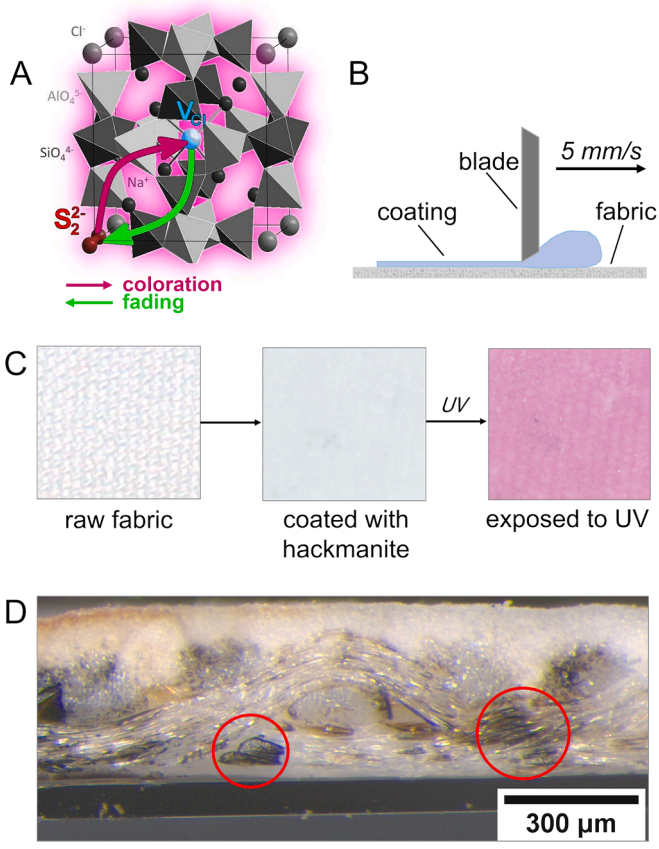


**Fig. 1.** Schematic illustrations of (A) hackmanite unit cell with specified electron trapping (purple arrow) and detrapping (green arrow) after exposure to proper wavelengths, and (B) the blading process. (C) Optical photos of raw fabric (left), fabric coated with a hackmanite-loaded film before (middle) and after (right) coloration. (D) A cross-section image of the sample taken with the optical microscope.

their reversible photochromism, also called tenebrescence (Fig. 1A) [1,3,32–38]. Compared with both organic and inorganic materials, these photochromic minerals offer a unique set of advantages by seamlessly combining the lightweight, flexible, and versatile traits of organic materials with the high thermal, chemical, and optical resistance typically found in inorganic substances [1,8,11,32,34,39,40]. This exceptional combination has already made hackmanites a material of great interest in the field of photochromism [11]. The photochromic mechanism exhibited by hackmanites originates from electronic transitions occurring within their robust crystal structure; therefore, the coloration and discoloration cycle can be repeated indefinitely [1,3,33,36,37]. Furthermore, a variety of colors (such as pink, purple, blue, or yellow) can be achieved by simple modifications to the synthesis formula and the compounds employed in the preparation of hackmanites with no toxic chemicals involved in the process [20]. The color intensity of hackmanite depends on both the intensity of UV radiation to which it is exposed and the density of switchable color centers inside the crystal lattice [1,20,32]. By observing the color changes in these minerals under sunlight, the intensity of UV radiation present in the environment can be estimated through, for example, UV index (UVI) measurements [1,8]. Furthermore, the coloring threshold wavelength of hackmanite aligns closely with the erythemal action spectrum of human skin, making these minerals particularly well suited for integration into accurate UV monitoring wearables [1].

One type of UV-sensitive yarn incorporating hackmanite was developed earlier when *Fang et al.* added the mineral to cellulose-based yarn during its initial production stages [8]. However, this method of incorporating photochromic material is limited to specific manufacturing techniques and does not apply to all commercially available fabrics. Furthermore, since recycling usually requires the separation of materials, a coating is likely easier for recycling processes than minerals permanently integrated into the yarn. In addition, the results showed that the hackmanite within the yarn was colored only with UV-C, which is practically nonexistent on the surface of the Earth since it is effectively absorbed by the ozone layer [8]. Previously reported hackmanite-containing coatings were applied on a polymethyl methacrylate-based sheet and incorporated toxic compounds, such as benzyl butyl phthalate and Triton X-100 [34,41]. For large-scale use, it is important to use only safe chemicals to ensure that the coatings are suitable for direct skin contact or exposure to the environment.

Herein, we introduce environmentally friendly hackmanite coatings that have been successfully applied to textile substrates, marking a novel contribution in the field. The performance of these fabrics was analyzed by assessing color changes upon UV exposure using color coordinates (Lab* color space) and reflectance spectroscopy. Next, we investigated the fading rate and fatigue resistance to evaluate the color reversal time and color stabilization through photochromic cycles. In addition, washing and flexibility tests were conducted to determine the mechanical resistance of the coating. These coloration properties were further utilized in the design of the proprietary phone app, Sensoglow, which was developed to calculate the UVI values based on the saturation level of the fabric. This study investigates how hackmanite-based UV-sensing wearables can monitor ambient UV exposure and warn users about UVI levels in real time. The aim is to prepare photochromic textiles that offer a compelling solution for enhancing the widespread accessibility of flexible photodetectors.

## 2. Experimental

### 2.1. Materials

Synthetic fabric (96 % polyester, 4 % elastane, 320 g/m$^2$ with a thickness of 350 µm) was bought from the Eurokangas store (Turku, Finland). Ethanol (>99.5 %) was purchased from Altia and ethyl methyl ketone (2-butanone, > 99.5 %) from VWR Chemicals. Tergitol (Type 15-S-9). Diisononyl cyclohexane-1,2-dicarboxylate (DINCH, Plastic

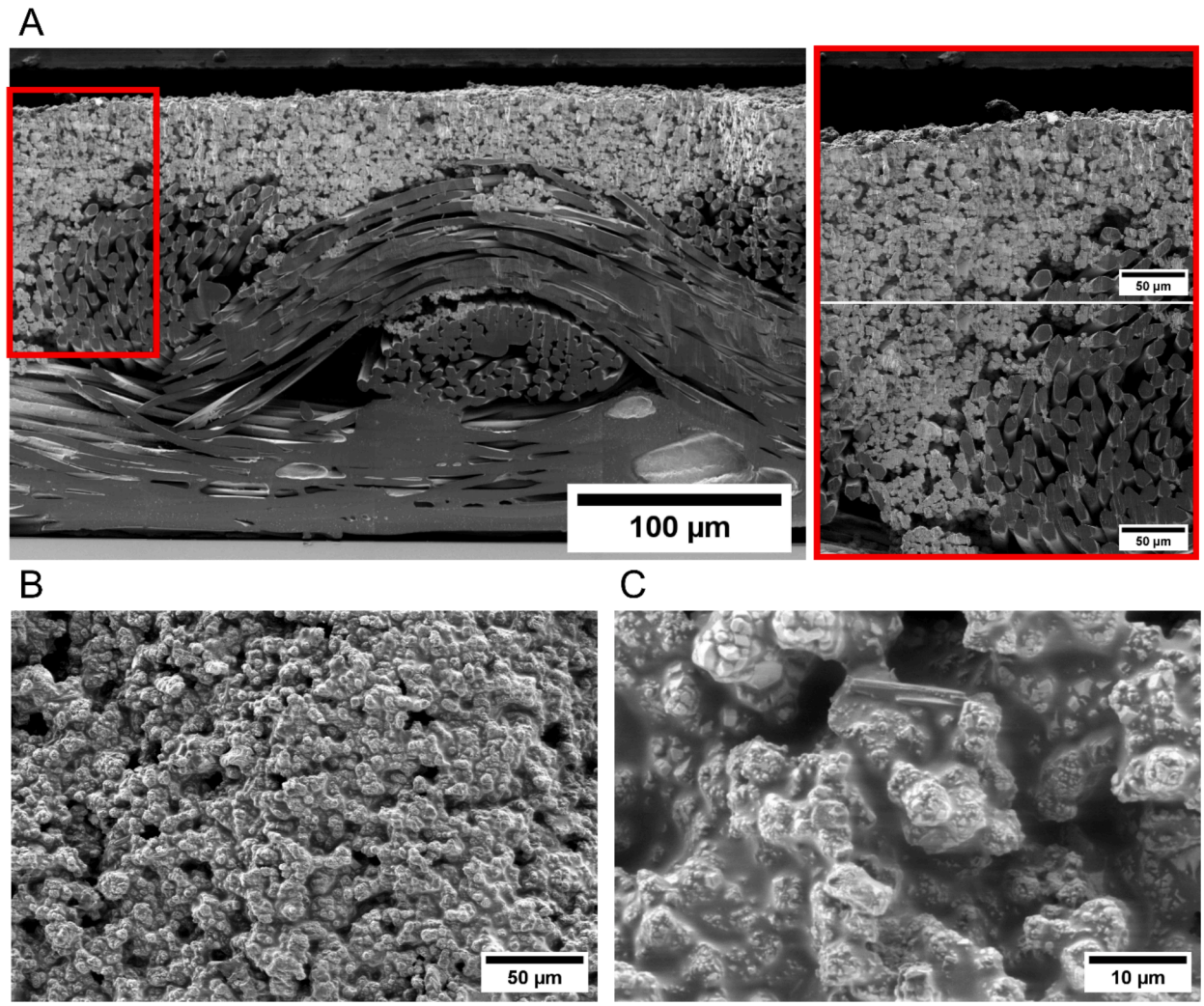


**Fig. 2.** SEM images of hackmanite-coated fabric, which showcase (A) cross-section highlighting the interface between the fabric (lower portion) and the coating (upper portion) of the sample with the zoomed elements on the right side, (B) a top-down view on a surface of the sample, and (C) a close-up view of the hackmanite crystals and their morphology.

additive 24) and polyvinyl butyral (PVB) were purchased from Sigma-Aldrich. All chemicals were used as received without further purification.

### 2.2. Synthesis of hackmanites

Hackmanite powder was synthesized following the procedure from [39]. According to [1,20], ($Na_8Al_6Si_6O_{24}(Cl,S)_2$) hackmanite absorbs UV-A, UV-B, and UV-C and changes its color from white to different shades of pink or purple. The X-ray diffraction (XRD) patterns of the hackmanite employed can be found in Supporting Information, Fig. S1.

### 2.3. Pretreatment of synthetic fabric

The synthetic fabric was cut into rectangles measuring 6 cm × 5 cm. The treatment began with a cleaning step in which the samples were immersed in a solution comprising 10 ml of nonionic detergent Decon90 and 90 ml of water. The mixture was stirred at 60 °C for 15 min to remove impurities from the fabric surface and subsequently rinsed with water [42]. Next, the fabrics were dried in an oven (Binder, model ED 56) at 50 °C for 12 h, and after this process, they were ready for further treatments.

### 2.4. Preparation of the photochromic coating

To fabricate a solid, flexible, and translucent film, 0.68 g of hackmanite powder, 0.25 g of ethanol, 0.51 g of 2-butanone, and 0.08 g of tergitol 15-S-9 were placed in a vessel with four grinding balls within a planetary mill (Philips Minimill Pw4018/00) and ground for 10 min at a speed setting of 1. Subsequently, 0.136 g of DINCH and 0.12 g of PVB were added to the paste, and the grinding continued for an additional 2 min at a speed setting of 5. Once the milling process was complete, the resulting mixture was quickly applied to the fabric with an Erichsen Coatmaster 510 film applicator with a blade movement speed of 5 mm/s, leading to a wet thickness of 315 µm (Fig. 1B). The relative humidity of the environment was maintained below 30 %. The freshly coated fabric was left to dry under a fume hood, and after 10 min, it was ready for further evaluation. Upon complete solvent evaporation, the finished film comprised approximately 73 % hackmanite [39].

### 2.5. Optical images and SEM analysis

The as-prepared sample was exposed to a UV-B lamp (Analytikjena UVM.57 handheld UV lamp 6 W with a wavelength of 302 nm) with 3 J/$cm^2$ (i.e., 30 kJ/$m^2$) to obtain the maximum coloration of the hackmanite coating. Photos of the sample were taken using a Canon EOS 250D camera before and after coloration. Next, a sample was prepared

to study both the surface morphology and the cross-sectional structure with an Apreo S field-emission scanning electron microscope (FE-SEM; Thermo Fisher Scientific, The Netherlands). The secondary electron micrographs were taken in low vacuum conditions using $H_2O$ with a chamber pressure of 100 Pa and an acceleration voltage of 2 kV. For the cross-section scanning electron microscope (SEM) analysis, the sample was fixed between a Si substrate and a thin glass cover with carbon cement and cut with an argon broad ion beam (BIB) mill (ArBlade 5000, Hitachi High-Technologies, Japan) using an ion beam acceleration voltage of 3.5 kV. To capture the morphology from a top-down perspective, a segment of the fabric was fixed onto copper tape without any additional preparation steps [42]. The cross-sectional structure of the fabric was further investigated using an Olympus SZX7 stereo microscope.

### 2.6. Color coordinates, reflectance, and light response measurements

The photochromic properties of the hackmanite-coated fabric were studied using both color coordinates (Lab* color space) and reflectance spectroscopy. To evaluate the color characteristics, the color coordinate values were obtained with the spectrophotometer Konica Minolta CM-2300 d with a D65 illuminant and a 10° observer with firmware version 3.16. The reflectance measurements were carried out with an Avantes AvaSpec HS-TEC spectrometer under a calibrated Ocean Optics LS-1 Cal light source with a geometry to minimize specular reflection coupled to a 1000 μm VIS/NIR 0.37NA PC04 optical fiber with parameters set to a value where the charge-coupled device detector would not saturate. In both measurements, the samples were irradiated with UV-B light (Analytikjena UVM.57 handheld UV lamp 6 W with a wavelength of 302 nm) at 3 J/cm$^2$ to obtain maximum coloration of the photochromic fabric. In addition, MgO powder served as the white reference in all reflectance measurements [42]. Data were collected before and after excitation. The coloration values in the figures are constructed from the difference reflectance spectra by numerically integrating the visible region (i.e., 400–800 nm) of the spectrum.

To conduct the rapid response performance measurements, the samples were exposed to UV lamps with wavelengths of 302 nm and 365 nm (Analytikjena UVLS-24 EL series UV lamp 4 W, 365 nm) with irradiance values of 5, 15, and 25 W/m$^2$, respectively, for a total duration of 10 min. The analysis was done with an Avantes AvaSpec ULS2048CL-EVO (302 nm) and an Avantes AvaSpec HS-TEC (365 nm) spectrometer coupled to a 1000 μm VIS/NIR 0.37NA PC04 optical fiber. The measurements were conducted under a 40 W incandescent lamp (for the reflectance measurements with the 302 nm lamp) and under a calibrated Ocean Optics LS-1 Cal light source (for the reflectance measurements with the 365 nm lamp) with a geometry to minimize specular reflection. Reflectance data were collected at set time intervals following the schedule shown in Fig. 3(C, D).

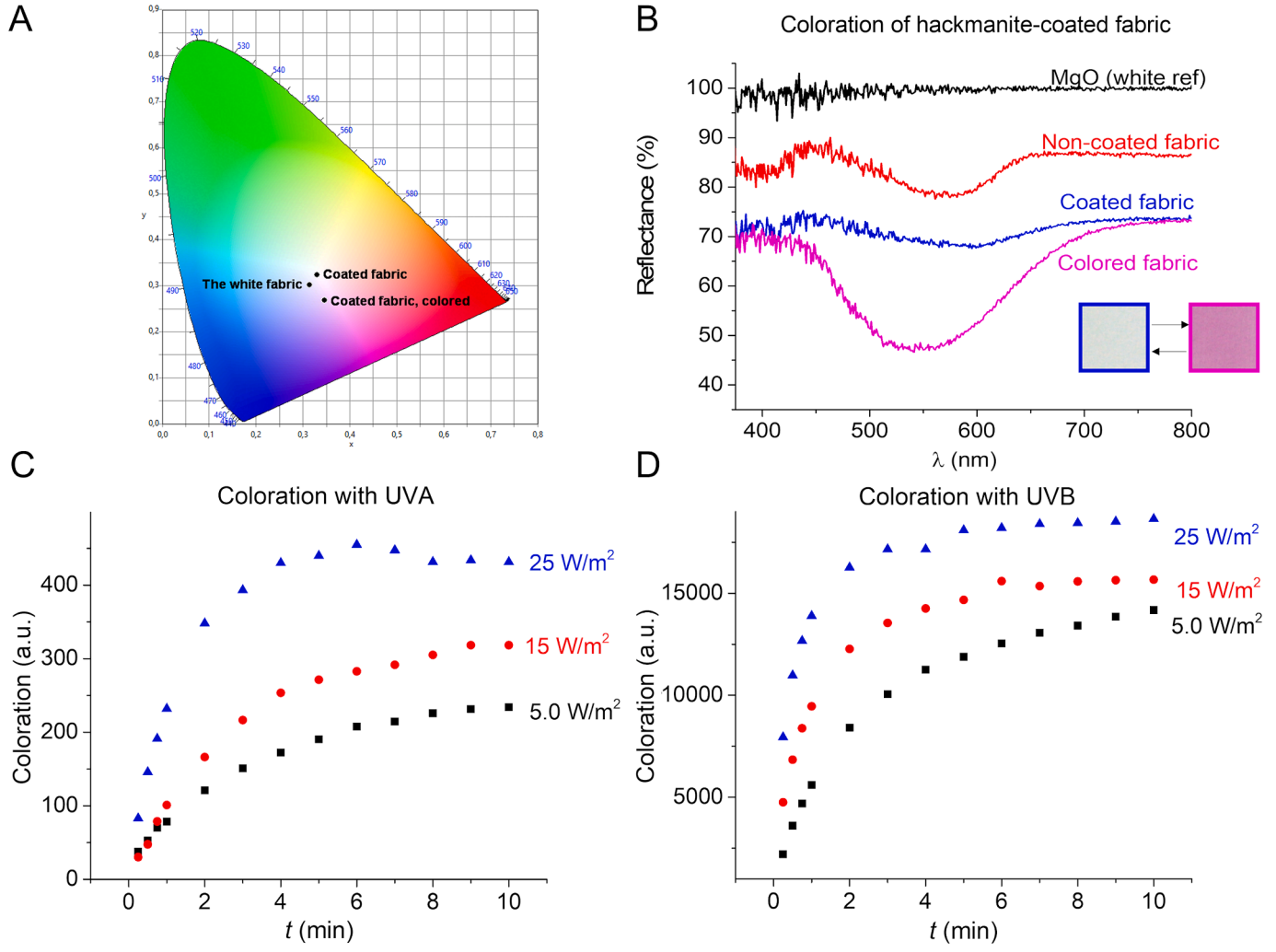


**Fig. 3.** (A) The distribution of the color of the hackmanite-coated fabric in the CIE-1931 color space, obtained using color coordinate values. (B) Reflectance measurements of the sample before and after UV-B exposure. (C) Coloration-to-time dependence plot of a sample upon UV-A and (D) UV-B exposure with specified irradiances of 25, 15, and 5 W/m$^2$, respectively.

### 2.7. Evaluation of fading rate and fatigue resistance

To evaluate the fading rate, the photochromic fabric was first exposed to UV-B light for a duration of 10 min, reaching the maximum coloration depth. Next, the colored fabric was placed under a solar simulator (AM1.5 solar spectrum, LOT QuantumDesign LS0500 with an Edinburgh Instruments 495 nm long pass filter) for a total duration of 70 min to bleach the coating fully. Reflectance spectra were measured using the setup employed for the rapid response performance measurements (see Section 2.6). The data were collected at set time intervals, following the schedule shown in Fig. 4(A, B). Furthermore, the fatigue resistance was assessed with the same setup used for the color characteristics evaluation (see Section 2.6). The photochromic coloration cycles were measured and analyzed with the color coordinate values of both maximum color depths and fully bleached states over 20 cycles.

### 2.8. UV index detection

To examine the color change dependent on UVI values in photochromic fabric, the samples were exposed to UV lamps emitting wavelengths of 302 nm and 365 nm simultaneously for a duration of 10 min, with UVI values set at 1, 3, 5, and 7. These UV wavelengths of 302 nm and 365 nm simulating UV-B and UV-A, respectively, were used to study the individual and specific responses of the material to the predominant UV wavelengths on the surface of the Earth [1]. The UVI values were measured using a Solarmeter® (Model 6.5 UV Index) UVI meter. Next, the color-changed segments of fabric were photographed using a camera (Canon EOS 250D) in constant light conditions. Subsequently, the G:G ratios (white:colored) of the RGB color space from the photos were utilized for calibrating the Sensoglow app [43]. This calibration enabled the app to identify UVI values by analyzing the coloration characteristics specific to the material. To further test the Sensoglow app, pictures were taken using an Oukitel WP 21 Ultra smartphone with Android 12.

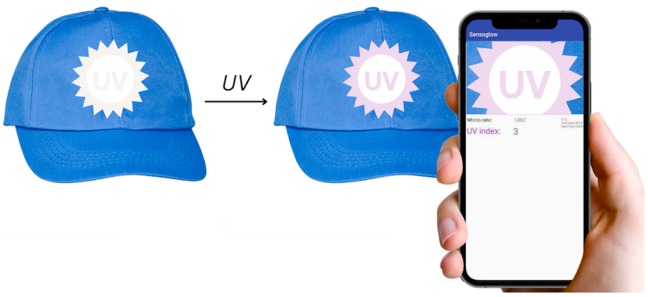


**Fig. 5.** The schematic illustration shows the practical application of hackmanite-loaded coatings used, for example, as prints on a cap. This example presents the functionality of photochromic fabric in indicating UVI through color intensity changes, which can be read and further analyzed with the proprietary Sensoglow app.

### 2.9. Evaluation of flexibility and washing durability

The flexibility of the fabric was tested using a Satra Upper Material Flexing Machine (model STM 407) for 500 flexing cycles. Further, the sample was investigated under a microscope (Tagarno, model Trend) to evaluate the cracks that appeared in the coating. Additionally, to visually assess the flexing of the sample, color patterns were applied onto the coating using a handmade photomask and a UV-B lamp (Fig. 6A) and subsequently captured with a Canon EOS 250D camera.

The washing durability test was conducted following DS/EN ISO 6330:2021 standard. The prepared photochromic fabric was first colored with a UV lamp with a wavelength of 302 nm (Analytikjena UVP UVLMS-38, 6 W 254/302/356 nm). Next, it was washed 5 times at a temperature of 30 °C for 30 min per cycle, using a standardized detergent at a quantity of 0.75 ml (see Supporting Info Section 2.4.). Following each washing cycle, the sample was dried at 50 °C in an oven

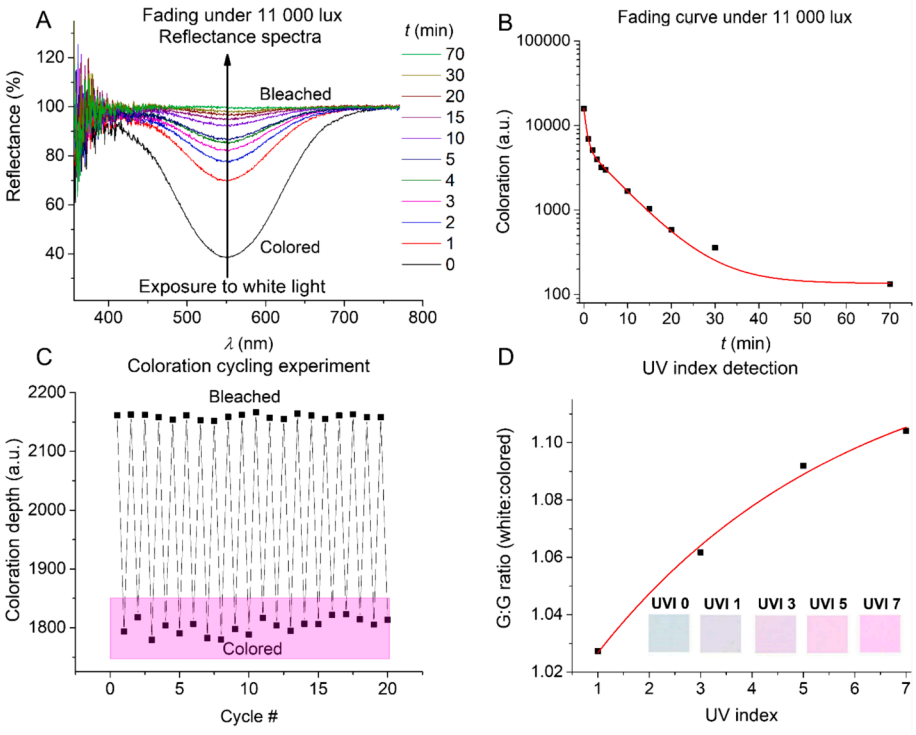


**Fig. 4.** (A) Fading process of the hackmanite-coated fabric upon exposure to white light (>495 nm), presented as reflectance spectrum and (B) the relation between the coloration intensity and fading time. (C) Color change cycles of the photochromic fabric upon exposure to UV-B and visible light spectrum, repeatedly. (D) Color intensity at different UV index values.

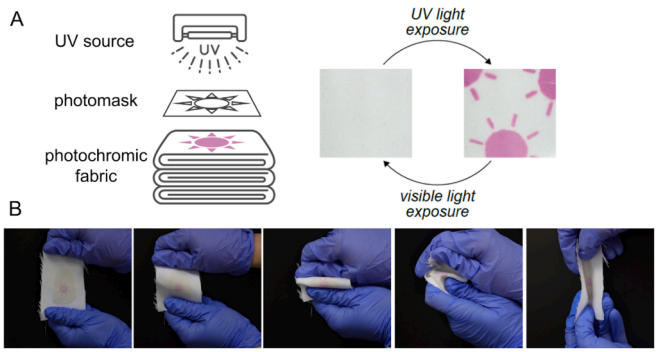


**Fig. 6.** (A) A schematic image displaying a sun-shaped pattern on the photochromic fabric (right), which can be done multiple times with a photomask and UV lamp (left). (B) A sun-shaped pattern fabricated on the photochromic fabric serves as a visual indicator to demonstrate the bending capacity of the coating.

(Binder, model FED 53) for 4 h to eliminate any residual moisture from the fabric under the DS/ISO 4484-1:2023 standard. Post-drying, the sample was weighed using a scale (Kern&Sohn GmbH, model ABT 220-5DNM) to assess any potential reduction in coating mass resulting from the washing process. Then, the sample was inspected using the microscope (Tagarno, model Trend) to analyze the difference in the physical appearance of the sample and the spectrophotometer (Konica Minolta) to evaluate the color fastness of the coating (see Section 2.6.).

## 3. Results and discussion

### 3.1. Optical and SEM images

The observed color change in Fig. 1C demonstrates the photochromic property of the coated fabric. Although UV-C wavelengths are more effective in the coloration of hackmanite, their presence on the Earth's surface is negligible [1,20,44]. Thus, maximum saturation was achieved with UV-B, the next most harmful UV radiation after UV-C. Upon exposure to UV-B, the sample swiftly transitions from its initial off-white state to a deep purple hue, confirming the successful preparation of the UV-responsive textile. Fig. 1D shows an optical image of the cross-sectional structure of the sample. The brown and black marks visible and highlighted with red circles in the image, indicate the carbonization of the sample due to the Ar ion beam damage used for intermittently cutting the sample with very low beam energy. Since the beam direction was from the fabric to the coating, the main damage occurred to the fabric, and by the time the beam reached the coating layer, no damage was visible.

The SEM images of the hackmanite-loaded coating on the synthetic fabric are presented in Fig. 2(A-C). In Fig. 2A, a cross-section image revealed a distinct interface between the coating and the fabric, demonstrating deeper penetration of the hackmanite-loaded solution beyond the surface layer. This enhanced penetration was likely due to the porous structure of the fabric and the presence of ethanol in the coating mixture. Ethanol, with its lower surface tension compared to water, could have infiltrated the hydrophobic matrix of synthetic fabrics more easily, thereby facilitating a deeper dispersion of hackmanites within the fabric matrix. In Fig. 2(B, C), the coating morphology was observed with hackmanite crystals covered in a thin layer of plasticizer. Despite the uneven structures and agglomerations of the crystals, their distribution within the coating remained uniform. Fig. S2(A-D) further explains what the chemical elements within the system were through backscattered electron (BSE) micrographs (Fig. S2(A, C)) and energy-dispersive X-ray spectroscopy maps (Fig. S2(B, D)).

### 3.2. Photochromism and performance of the hackmanite-coated fabric: color coordinates, reflectance, light response measurements

Fig. 3A shows the chromaticity diagram within the CIE-1931 color space, with three points representing the uncoated white fabric (used as the substrate), the coated fabric, and the color-saturated coated fabric under UV-B light. The reflectance spectra were used to show the photochromic effect of the sample, as demonstrated in Fig. 3B. Without UV irradiation, the hackmanite-coated fabric shows only a uniform decrease throughout the whole visible reflectance spectrum. There is a visible absorption band at ~580 nm, which appeared due to the hackmanite layer being slightly transparent, meaning that the yellow absorption band of the fabric itself is partly visible in the spectrum. The color is characterized by a broad absorption band in the green light region (~540 nm) of the electromagnetic spectrum, which is also easily observed as a purple color, even by the naked eye [1].

Given that UV-A and UV-B wavelengths primarily determine the UVI, time-response measurements were conducted following UV-A and UV-B light exposure, as shown in Fig. 3(C, D). Overall, assessing the light response time is crucial for identifying UVI in photodetectors, since a higher UV photon flux translates to a higher stochastic risk of developing skin diseases. As observed for both UV-A and UV-B, the coating changed its color after just 15 s of light exposure, with a significant color difference noted under UV-B—four times faster than a coloration rate of a photochromic cotton fabric reported in a similar study [2]. Fig. 3(C, D) illustrates the strong correlation between different levels of UV light exposure and the resulting visible color shifts, and the coloration was dependent on the UV dose (see Supporting Info Fig. S3). At low UV doses, there is a linear correlation between UV exposure and coloration, while at high doses, the coloration saturates. Notably, lower UV intensity correlates with slower color changes, aligning with expectations due to the reduced probability of UV photons generating color centers. Consequently, when the UV light intensity increased, the color changed faster. The coloration obtained after 10 min of UV exposure remained relatively stable, suggesting that saturation had been reached and that the color had reached the deepest tone; hence, this time value was utilized in performing the other measurements. In Fig. 3C, at an intensity of 25 $W/m^2$ after 7 min, a slight occurrence of solarization was observed, indicating a loss of coloration after reaching a sufficiently high dose [44].

### 3.3. Evaluation of fading rate and fatigue resistance

If the colored hackmanite-coated fabric is placed next to the window on a sunny day, it will gradually fade over time until the purple color fully disappeared [36]. Such an experiment was conducted on the 21st of May 2024 in Turku, Finland, with the window facing southeast. The result indicated a bleaching time of around 30 min on a sunny day (see Supporting Info Fig. S4). However, to standardize the conditions of the bleaching process, the fully saturated coated fabric was exposed to a solar lamp with a 495 nm long-pass filter, as specified in Section 2.7. The results related to the evaluation of the fading time are shown in Fig. 4(A, B). Overall, assessing the fading performance is necessary to determine the reusability of the UV-sensing fabric without inducing significant delays [11]. Thus, the sample was analyzed with reflectance spectra (Fig. 4A) and a fading curve (Fig. 4B and S5A). In Fig. 4A, the reflectance spectra can be seen to rise toward the original 100 % level (a bleached coating that was set as the white reference) as a function of visible light exposure. After reaching an exposure time of 50 min, the spectrum matched the values of the uncolored fabric, meaning the complete restoration to its original state. A similar trend can be observed in the fading curve (Fig. 4B and S5A), which plateaued at 50 min and remained stable until the end of the measurement (70 min). Notably, the resultant time was double the speed of, for example, a photochromic matrix of polyacrylic acid and sodium deca-tungstate, which required 2 h to return to its initial colorless state [11].

Moreover, synthetic hackmanites have been reported to remain stable through a minimum of 13 cycles without noticeable effects on coloration efficiency [3]. In this study, the results of the fatigue resistance test demonstrated that the photochromic effect remained stable through a minimum of 20 cycles, with the color saturation intensity maintained over time, as presented in Fig. 4C. The fluctuation of values in the colored coating is due to natural variation when measuring the spectra. This photochromic cycle plot shows that hackmanite exhibited greater coloration stability compared to other materials. For instance, the tungsten-oxide-based matrix experienced a color saturation intensity loss of approximately 10 % after only 10 photochromic cycles [31]. Similarly, the spiropyran-based photochromic yarn demonstrated gradual photobleaching throughout 10 cycles [29]. This high fatigue resistance of hackmanites is due to the mineral nature of the material. Since the coloration mechanism involves electronic transitions within short distances inside the strong crystal lattice, tenebrescence is protected by the mineral structure itself. There are minute geometrical changes in the color center and its accompanying disulfide ion, but the structural alteration is subtle enough to happen without any chemical bonds being broken during the coloration and bleaching processes [3].

### 3.4. UV index detection

The UVI serves as an international standard established by the World Health Organization (WHO) to measure the intensity of sunburn-inducing UV radiation. Its primary purpose is to enable real-time monitoring of UV irradiation levels in outdoor environments [16,29,45]. Generally, a UVI above 3 indicates moderate chances of sunburn, from 6 to 7 signifies a heightened risk of sunburn, while a value exceeding 8 indicates danger [29,45]. Hence, the WHO recommends covering up with long sleeves or using sunscreen when the UVI is between 3 and 7, while for UVI equal to 8 or more, it is strongly advised to avoid any outdoor activities [46]. However, obtaining accurate UVI measurements for a specific region or country (e.g., a holiday destination) through Internet search engines can be challenging due to various factors, including language barriers and station names [16]. More importantly, UV radiation levels (i.e., the index values) vary throughout the day and by locality, which highlights the importance of continuous monitoring [45]. Highly conveniently, the coloring threshold of synthetic hackmanites matches the erythemal action spectrum of human skin [1]. Therefore, the sample was tested for UVI values of 0, 1, 3, 5, and 7–0 serving as a reference value and 7 as the upper limit above which WHO recommends staying indoors. The results shown in Fig. 4D and S4B demonstrate that hackmanite-coated fabrics can serve as effective UVI detectors. The noticeable color change in the fabric could be easily detected even by inexperienced users, meaning that a mere visual inspection of the fabric already provides a simple method of assessing real-time UVI levels. In Fig. 4D, the coloration occurred even at a UVI below 3–3 being the commonly recognized threshold for taking preventive measures against sunburn, as mentioned before [1,45]. However, to deliver more accurate information, we suggest using a mobile app that can monitor the color change of hackmanite-containing coatings, such as Sensoglow, as presented in Fig. 5. The smartphone app eliminates reliance on visual color judgment, addressing discrepancies in, for example, printed UV indicator color references [20]. A screenshot of the Sensoglow app is presented in Fig. S6. The working principle of the application consists of taking a photo of a coating that has received UV radiation and comparing it to a non-colored one and a fully colored one (which may be colored to a certain UVI value, e.g., 7). The coloration values are ratios obtained by calculating the difference between the green channel values of each measurement spot. In addition, the app can be updated to accommodate other colors or hues of hackmanites used in sensor fabrication [20,44]. It is important to note that since a major part of sunlight consists of visible light, which is an essential agent that bleaches the coloration of hackmanite, in any practical application, a shortpass filter should be used, as reported in [1]. These results were obtained without the presence of visible light, therefore, in bright sunlight, the colors would be less intense.

### 3.5. Evaluation of flexibility and washing durability

The flexibility of the coating was tested through a series of 500 flex cycles until failure, and breakages were observed at two distinct points on the surface, as shown in Fig. S7. In addition, the sun-shaped pattern was temporarily imprinted onto the photochromic coating to serve as a visual reference point. It was observed that the fabric flexed easily in all directions, as presented in Fig. 6(A, B).

For wearables, washing durability is an important performance metric that directly impacts the life cycle of the garment [11]. After having undergone 5 complete cycles of washing, the tested sample exhibited a loss of 0.18 g from its initial mass, which was approximately 3 % of the total mass (Fig. S8 and Table S1). Notably, the highest mass loss occurred after the first washing cycle, and these values decreased significantly with subsequent cycles. The first washing likely removed all loose particles, such as dust or other impurities accumulated on the sample while processing. Moreover, the slight errors in the mass differences are due to a more humid environment existing on the day of the measurement; the presence of additional moisture in the system influenced the final mass of the sample. The reflectance measurement showed a gradual change in the coloration of the coating toward white hue after each washing cycle (Fig. S9). In addition, there were no significant changes in coloration depth after washing, demonstrating the resistance of hackmanite to this process. In contrast, in the washing fastness tests conducted on photochromic bacterial cellulose material, the color difference between cycles gradually decreased, indicating a slow loss of coloration [47]. Finally, it was noted that following the fifth washing cycle, visible breakages appeared on the surface of the coating (Fig. S8). Five washing cycles are already sufficient for some pieces of clothing that are washed infrequently, such as caps.

## 4. Conclusion

In this study, we successfully fabricated hackmanite-coated fabrics with UV-sensing characteristics. Under UV-B and UV-A irradiation exposure, the fabric swiftly transitioned from its initial white color to a deep purple within 15 s, demonstrating its rapid response to UV irradiation. Subsequent exposure to white light led to a complete reversal of coloration in approximately 50 min, which was significantly faster than the other reported photochromic fabrics. Additionally, fatigue resistance, evaluated across 20 photochromic cycles, exhibited consistent color saturation throughout the assessment. This result proved that the coloration stability of hackmanite-based fabric lasts longer when compared with alternative photochromic materials, such as tungstate-or spiropyran-based dyes, which experienced saturation loss after just 10 cycles. Furthermore, the coating demonstrated resilience through 5 washing cycles and 500 flex cycles before exhibiting surface breakage, which means it can serve effectively in the form of, for example, a photochromic print on a cap.

Moreover, the hackmanite-coated fabric demonstrated the ability to detect UVI values at levels below the value of 3, which is essential for effective sunburn prevention measures. For easy and accurate reading of UVI, we suggested using a proprietary phone app, Sensoglow, which was compatible with the coloration change of the sample.

These findings have shown the potential of hackmanite-based wearable UV sensors to address the need for more accessible and widespread photodetectors. In particular, where UV monitoring is crucial and UVI may exceed 7, these sensors are valuable for preventing sunburn and the possible implications of too-long sun exposure.

## CRediT authorship contribution statement

**Alicja Lawrynowicz:** Conceptualization, Methodology, Formal

analysis, Investigation, Data Curation, Writing – original draft, Visualization. **Sami Vuori:** Writing – original draft, Visualization, Software, Methodology, Investigation, Formal analysis, Data curation, Conceptualization. **Emilia Palo:** Writing – review & editing, Supervision. **Mathias Winther:** Investigation. **Mika Lastusaari:** Writing – review & editing, Supervision, Resources. **Kati Miettunen:** Writing – review & editing, Supervision, Resources, Project administration, Funding acquisition, Conceptualization.

## Declaration of competing interest

The authors declare the following financial interests/personal relationships which may be considered as potential competing interests: Alicja Lawrynowicz reports financial support was provided by NordForsk. Mika Lastusaari has patent licensed to TURUN YLIOPISTO. If there are other authors, they declare that they have no known competing financial interests or personal relationships that could have appeared to influence the work reported in this paper.

## Data availability

Data will be made available on request.

## Acknowledgments

This work was supported by NordForsk, Norway, through funding for the *Nordic network on smart light-conversion textiles beyond electric circuits,* project number 103894. We acknowledge the Materials Research Infrastructure (Mari), University of Turku, Finland and specifically thank the Department of Physics and Astronomy, University of Turku, Finland, for access and support with the SEM and BIB facilitiesand Dr. Ermei Mäkilä for valuable help in the SEM analysis. Further, we thank Dr. Hannah Byron for providing the first batch of hackmanite and Rustem Nizamov for helping with photographing the samples. We also thank VIA University College, Denmark, for the possibility of using the testing facilities, and special thanks to Dr. Anne Louise Bang and Poul-Erik Jørgensen for their support.

## Appendix A. Supplementary data

Supplementary data to this article can be found online at https://doi.org/10.1016/j.cej.2024.153069.

## References

[1] I. Norrbo, A. Curutchet, A. Kuusisto, J. Mäkelä, P. Laukkanen, P. Paturi, T. Laihinen, J. Sinkkonen, E. Wetterskog, F. Mamedov, T. Le Bahers, M. Lastusaari, Solar UV index and UV dose determination with photochromic hackmanites: from the assessment of the fundamental properties to the device, Mater. Horiz. 5 (2018) 569–576, https://doi.org/10.1039/C8MH00308D.

[2] J. Fan, B. Bao, Z. Wang, H. Li, Y. Wang, Y. Chen, W. Wang, D. Yu, Flexible, switchable and wearable image storage device based on light responsive textiles, Chem. Eng. J. 404 (2021) 126488, https://doi.org/10.1016/j.cej.2020.126488.

[3] P. Colinet, H. Byron, S. Vuori, J.-P. Lehtiö, P. Laukkanen, L. Van Goethem, M. Lastusaari, T. Le Bahers, The structural origin of the efficient photochromism in natural minerals, Proc. Natl. Acad. Sci. 119 (2022) e2202487119, https://doi.org/10.1073/pnas.2202487119.

[4] A. Curutchet, T. Le Bahers, Modeling the photochromism of S-doped sodalites using DFT, TD-DFT, and SAC-CI methods, Inorg. Chem. 56 (2017) 414–423, https://doi.org/10.1021/acs.inorgchem.6b02323.

[5] M. Irie, Photochromism: Memories and Switches Introduction, Chem. Rev. 100 (2000) 1683–1684, https://doi.org/10.1021/cr980068l.

[6] S. Kawata, Y. Kawata, Three-dimensional optical data storage using photochromic materials, Chem. Rev. 100 (2000) 1777–1788, https://doi.org/10.1021/cr980073p.

[7] Y.-J. Ma, J.-X. Hu, S.-D. Han, J. Pan, J.-H. Li, G.-M. Wang, Photochromism and photomagnetism in crystalline hybrid materials actuated by nonphotochromic units, Chem. Commun. 55 (2019) 5631–5634, https://doi.org/10.1039/C9CC02229E.

[8] W. Fang, E. Sairanen, S. Vuori, M. Rissanen, I. Norrbo, M. Lastusaari, H. Sixta, UV-sensing cellulose fibers manufactured by direct incorporation of photochromic minerals, ACS Sustain. Chem. Eng. 9 (2021) 16338–16346, https://doi.org/10.1021/acssuschemeng.1c05938.

[9] H. Li, J. Zhou, J. Zhao, Fabrication of dual-functional cellulose nanocrystals/fluorinated polyacrylate containing coumarin derivatives by RAFT-assisted Pickering emulsion polymerization for self-healing application, Appl. Surf. Sci. 614 (2023) 156180, https://doi.org/10.1016/j.apsusc.2022.156180.

[10] M. Lastusaari, I. Norrbo, Synthetic material for detecting ultraviolet radiation and/or X-radiation, WO 2017/194834 A1, 2017.

[11] B. Bao, J. Fan, Z. Wang, Y. Wang, W. Wang, X. Qin, D. Yu, Sodium deca-tungstate /polyacrylic acid self-assembled flexible wearable photochromic composite fabric for solar UV detector, Compos. Part B Eng. 202 (2020) 108464, https://doi.org/10.1016/j.compositesb.2020.108464.

[12] Z. He, W. Wang, J. Fan, B. Bao, X. Qin, D. Yu, Photochromic microcapsules anchored on cotton fabric by layer-by-layer self-assembly method with erasable property, React. Funct. Polym. 157 (2020) 104762, https://doi.org/10.1016/j.reactfunctpolym.2020.104762.

[13] S. Fan, Y. Lam, J. Yang, X. Bian, J.H. Xin, Development of photochromic poly (azobenzene)/PVDF fibers by wet spinning for intelligent textile engineering, Surf. Interfaces 34 (2022) 102383, https://doi.org/10.1016/j.surfin.2022.102383.

[14] A.P. Periyasamy, M. Viková, M. Vik, Preparation of photochromic isotactic polypropylene filaments: influence of drawing ratio on their optical, thermal and mechanical properties, Text. Res. J. 90 (2020) 2136–2148, https://doi.org/10.1177/0040517520912037.

[15] X. Cui, L. Wang, Q. Dong, W. Liang, S. Zhao, Synthesis and characterization of a UV-resistant ZnO/pyrophyllite nanocomposite prepared by solid-state reaction method, Ceram. Int. 48 (2022) 34084–34091, https://doi.org/10.1016/j.ceramint.2022.08.165.

[16] A.W. Schmalwieser, J. Gröbner, M. Blumthaler, B. Klotz, H. De Backer, D. Bolsée, R. Werner, D. Tomsic, L. Metelka, P. Eriksen, N. Jepsen, M. Aun, A. Heikkilä, T. Duprat, H. Sandmann, T. Weiss, A. Bais, Z. Toth, A.-M. Siani, L. Vaccaro, H. Diémoz, D. Grifoni, G. Zipoli, G. Lorenzetto, B.H. Petkov, A.G. Di Sarra, F. Massen, C. Yousif, A.A. Aculinin, P. Den Outer, T. Svendby, A. Dahlback, B. Johnsen, J. Biszczuk-Jakubowska, J. Krzyscin, D. Henriques, N. Chubarova, P. Kolarž, Z. Mijatovic, D. Groselj, A. Pribullova, J.R.M. Gonzales, J. Bilbao, J.M. V. Guerrero, A. Serrano, S. Andersson, L. Vuilleumier, A. Webb, J. O'Hagan, UV Index monitoring in Europe, Photochem. Photobiol. Sci. 16 (2017) 1349–1370, https://doi.org/10.1039/c7 pp00178a.

[17] W. Liu, W. Cheng, M. Zhou, B. Xu, P. Wang, Q. Wang, Y. Yu, Construction of multifunctional UV-resistant, antibacterial and photothermal cotton fabric via silver/melanin-like nanoparticles, Cellulose 29 (2022) 7477–7494, https://doi.org/10.1007/s10570-022-04740-1.

[18] Y. Zhang, M. Peng, Y. Liu, T. Zhang, Q. Zhu, H. Lei, S. Liu, Y. Tao, L. Li, Z. Wen, X. Sun, Flexible self-powered real-time ultraviolet photodetector by coupling triboelectric and photoelectric effects, ACS Appl. Mater. Interfaces 12 (2020) 19384–19392, https://doi.org/10.1021/acsami.9b22572.

[19] M. Aldib, R.M. Christie, Textile applications of photochromic dyes. Part 4: application of commercial photochromic dyes as disperse dyes to polyester by exhaust dyeing, Color. Technol. 127 (2011) 282–287, https://doi.org/10.1111/j.1478-4408.2011.00308.x.

[20] H.C. Byron, C. Swain, P. Paturi, P. Colinet, R. Rullan, V. Halava, T. Le Bahers, M. Lastusaari, Highly tuneable photochromic sodalites for dosimetry, security marking and imaging, Adv. Funct. Mater. (2023) 2303398, https://doi.org/10.1002/adfm.202303398.

[21] Z. He, B. Bao, J. Fan, W. Wang, D. Yu, Photochromic cotton fabric based on microcapsule technology with anti-fouling properties, Colloids Surf. Physicochem. Eng. Asp. 594 (2020) 124661, https://doi.org/10.1016/j.colsurfa.2020.124661.

[22] X. Wang, W. Wang, Y. Li, Y. Wang, Preparation of tungsten-based polyvinyl alcohol waterborne coating and development of photochromic composite fabric, Macromol. Mater. Eng. 306 (2021) 2100540, https://doi.org/10.1002/mame.202100540.

[23] T.J. Adams, A.R. Brotherton, J.A. Molai, N. Parmar, J.R. Palmer, K.A. Sandor, M. G. Walter, Obtaining reversible, high contrast electrochromism, electrofluorochromism, and photochromism in an aqueous hydrogel device using chromogenic thiazolothiazoles, Adv. Funct. Mater. 31 (2021) 2103408, https://doi.org/10.1002/adfm.202103408.

[24] S. Sarker, D.K. Macharia, Y. Zhang, Y. Zhu, X. Li, M. Wen, R. Meng, N. Yu, Z. Chen, M. Zhu, Synthesis of $MnO_2$ –Ag nanojunctions with plasmon-enhanced photocatalytic and photothermal effects for constructing rewritable mono-/multi-color fabrics, ACS Appl. Mater. Interfaces 14 (2022) 5545–5557, https://doi.org/10.1021/acsami.1c19731.

[25] T.H. Fleisch, G.J. Mains, An XPS study of the UV reduction and photochromism of MoO3 and WO3, J. Chem. Phys. 76 (1982) 780–786, https://doi.org/10.1063/1.443047.

[26] S. Nigel Corns, S.M. Partington, A.D. Towns, Industrial organic photochromic dyes, Color. Technol. 125 (2009) 249–261, https://doi.org/10.1111/j.1478-4408.2009.00204.x.

[27] S. Kumar, S. Soni, W. Danowski, I.F. Leach, S. Faraji, B.L. Feringa, P. Rudolf, R. C. Chiechi, Eliminating Fatigue in Surface-Bound Spiropyrans, J. Phys. Chem. C 123 (2019) 25908–25914, https://doi.org/10.1021/acs.jpcc.9b05889.

[28] Y. Qi, J. Fan, Y. Chang, Y. Li, B. Bao, B. Yan, H. Li, P. Cong, Smart photochromic fabric prepared via thiol-ene click chemistry for image information storage applications, Dyes Pigments 193 (2021) 109507, https://doi.org/10.1016/j.dyepig.2021.109507.

[29] Y. Zheng, W. Panatdasirisuk, J. Liu, A. Tong, Y. Xiang, S. Yang, Patterned, wearable UV Indicators from electrospun photochromic fibers and yarns, Adv. Mater. Technol. 5 (2020) 2000564, https://doi.org/10.1002/admt.202000564.

[30] J. Fan, B. Bao, Z. Wang, R. Xu, W. Wang, D. Yu, High tri-stimulus response photochromic cotton fabrics based on spiropyran dye by thiol-ene click chemistry, Cellulose 27 (2020) 493–510, https://doi.org/10.1007/s10570-019-02786-2.
[31] B. Bao, J. Fan, W. Wang, D. Yu, Novel linen/polyethyleneimine/sodium decadecanate photochromic fabric prepared by layer-by-layer self-assembly method, Cellulose 27 (2020) 6591–6602, https://doi.org/10.1007/s10570-020-03234-2.
[32] I. Norrbo, Synthetic hackmanites and their optical properties – from theory to applications, University of Turku (2019). https://urn.fi/URN:ISBN:978-951-29-7624-9.
[33] D.B. Medved, Hackmanite and its tenebrescent properties, Am. Mineral. 39 (1954) 615–629.
[34] S. Vuori, P. Colinet, J.-P. Lehtiö, A. Lemiere, I. Norrbo, M. Granström, J. Konu, G. Ågren, P. Laukkanen, L. Petit, A.J. Airaksinen, L. Van Goethem, T. Le Bahers, M. Lastusaari, Reusable radiochromic hackmanite with gamma exposure memory, Mater. Horiz. 9 (2022) 2773–2784, https://doi.org/10.1039/D2MH00593J.
[35] E.F. Williams, W.G. Hodgson, J.S. Brinen, Synthetic photochromic sodalite, J. Am. Ceram. Soc. 52 (1969) 139–144, https://doi.org/10.1111/j.1151-2916.1969.tb11200.x.
[36] I. Norrbo, P. Gluchowski, I. Hyppänen, T. Laihinen, P. Laukkanen, J. Mäkelä, F. Mamedov, H.S. Santos, J. Sinkkonen, M. Tuomisto, A. Viinikanoja, M. Lastusaari, Mechanisms of Tenebrescence and Persistent Luminescence in Synthetic Hackmanite $Na_8Al_6Si_6O_{24}$ ($Cl_2$ S) 2, ACS Appl. Mater. Interfaces 8 (2016) 11592–11602, https://doi.org/10.1021/acsami.6b01959.
[37] R.D. Krnr, The luminescence and tenebrescence of natural and synthetic sodalite, Am. Mineral. 40 (1955).
[38] J.A. Armstrong, M.T. Weller, Structural observation of photochromism, Chem. Commun. (2006) 1094, https://doi.org/10.1039/b517715d.
[39] S. Vuori, Reversible photochromism of synthetic hackmanites in radiation detection and quantification, University of Turku (2023). https://urn.fi/URN:ISBN:978-951-29-9280-5.
[40] C. Agamah, S. Vuori, P. Colinet, I. Norrbo, J.M. De Carvalho, L.K. Okada Nakamura, J. Lindblom, L. Van Goethem, A. Emmermann, T. Saarinen, T. Laihinen, E. Laakkonen, J. Lindén, J. Konu, H. Vrielinck, D. Van Der Heggen, P.F. Smet, T. L. Bahers, M. Lastusaari, Hackmanite—the natural glow-in-the-dark material, Chem. Mater. 32 (2020) 8895–8905, https://doi.org/10.1021/acs.chemmater.0c02554.
[41] S. Vuori, P. Colinet, I. Norrbo, R. Steininger, T. Saarinen, H. Palonen, P. Paturi, L.C. V. Rodrigues, J. Göttlicher, T. Le Bahers, M. Lastusaari, Detection of X-ray doses with color-changing hackmanites: mechanism and Application, Adv. Opt. Mater. 9 (2021), https://doi.org/10.1002/adom.202100762.
[42] A. Lawrynowicz, E. Palo, R. Nizamov, K. Miettunen, Self-cleaning and UV-blocking cotton – Fabricating effective ZnO structures for photocatalysis, J. Photochem. Photobiol. Chem. 450 (2024) 115420, https://doi.org/10.1016/j.jphotochem.2023.115420.
[43] S. Vuori, T. Laine, I. Norrbo, J. Holvitie, M. Lastusaari, An Android Application for Determining UV Index and UV Dose from Hackmanite., (2024).
[44] S. Vuori, H. Byron, I. Norrbo, M. Tuomisto, M. Lastusaari, Photochromic photography with hackmanite obtained by large-scale synthesis, J. Ind. Eng. Chem. 120 (2023) 361–373, https://doi.org/10.1016/j.jiec.2022.12.043.
[45] E. Rehfuess, Global solar UV index: a practical guide, World Health Organization, Geneva, Switzerland, 2002.
[46] D.-H. Park, S.-T. Oh, J.-H. Lim, Development of a UV index sensor-based portable measurement device with the EUVB ratio of natural light, Sensors 19 (2019) 754, https://doi.org/10.3390/s19040754.
[47] J. Li, Y. Liu, Z. Gu, P. Sun, K. Liu, D. Xu, C. Gao, W. Xu, Scalable, green, flexible photochromic bacterial cellulose for multicolor switching, photo-patterning, and daily sunlight UV monitoring, Small (2024) 2309514, https://doi.org/10.1002/smll.202309514.